Properties of finite nuclei in the modified quark-meson coupling model

H. Müller
TRIUMF, 4004 Wesbrook Mall, Vancouver, British Columbia, Canada V6T 2A3
(Received 23 October 1997)

The modified quark-meson coupling (MQMC) model is applied to describe the properties of finite nuclei. The concept of a density-dependent bag constant is used to calibrate the model at equilibrium nuclear matter density. By a redefinition of the scalar meson field, the MQMC model can be cast in a form similar to a quantum hydrodynamics (QHD) type mean-field model. Binding energies, charge radii, and single-particle spectra of spherical nuclei are analyzed and compared with QHD calculations and with results based on the original quark-meson coupling model. The accurate reproduction of the effective nucleon mass in the MQMC model leads to a realistic description of single-particle spectra and spin-orbit splittings. Changes of the internal quark structure of the nucleon in the nuclear environment are also discussed. [S0556-2813(98)04704-9]

PACS number(s): 24.85.+p, 21.60.−n, 21.10.−k, 12.39.Ba

I. INTRODUCTION

Although quantum chromodynamics is believed to be the fundamental theory of strong interactions, low- and medium-energy nuclear phenomenology is successfully described in terms of hadronic degrees of freedom. Besides the fundamental question of how this picture emerges from the underlying theory, theoretical challenges arise in phenomena which reveal the quark structure of hadrons, for example, the prominent EMC effect which indicates medium modifications of the internal structure of the nucleon [1]. Moreover, hadronic models are often extrapolated into regimes of high density and temperature to extract the nuclear equation of state, which is the basic ingredient in many astrophysical applications and in microscopic models of energetic nucleus-nucleus collisions. One can expect that under these extreme conditions quark degrees of freedom become important.

At present rigorous studies of QCD are restricted to matter systems at high temperature and zero baryon density. Because of the nonperturbative features of this theory, it is very difficult to derive predictions at energy scales relevant for low- and medium-energy nuclear phenomenology.

Thus, there is a need to build models which incorporate quark-gluon degrees of freedom and which help to bridge the gap between nuclear phenomenology and the underlying physics of strong interactions. Such models are necessarily crude since the study of the nuclear many-body problem on the fundamental level is intractable. However, it is important that the new models respect established results which are successfully described in the hadronic framework.

Recently, much effort has been devoted to the study of effective models for low-energy strong interactions. Typical examples are Nambu–Jona-Lasinio (NJL) type soliton models [2]. Although these models successfully describe the properties of single hadrons, it is not clear if basic features of nuclear phenomenology, such as saturation of nuclear matter, can be reproduced properly. Because the nucleons have to be built in these models, it is difficult to perform the step from a single-nucleon to a many-nucleon system [3].

The quark-meson coupling (QMC) model proposed by Guichon [4] provides a simple and attractive framework to incorporate quark degrees of freedom in the study of nuclear many-body systems. In the QMC model nucleons arise as nonoverlapping MIT bags interacting through meson mean fields. The model has been applied to a variety of problems in nuclear physics. It was shown that it describes the saturation properties of nuclear matter [5–10] and that it gives a fair description of the bulk properties of finite nuclei [11–15]. The model was extended to include hyperons [16] and applied to studies of hypernuclei [17,18].

Although it provides a simple and intuitive framework to describe the basic features of nuclear systems in terms of quark degrees of freedom, the QMC model has a serious shortcoming. It predicts much smaller scalar and vector potentials than obtained in successful hadronic models [6,8,9]. As a consequence the nucleon mass is too high and the spin-orbit force is too weak to explain spin-orbit splittings in finite nuclei [12–14].

A well-established framework for relativistic hadronic models is provided by quantum hadrodynamics (QHD) [19]. Numerous calculations have established that relativistic mean-field models based on QHD lead to a realistic description of the bulk properties of finite nuclei and nuclear matter [19]. A very compelling feature of QHD has been the reproduction of spin-orbit splittings in finite nuclei. One of the key observations in their success is that nucleon propagation in the nuclear medium is described by a Dirac equation featuring large scalar and vector potentials.

Recently, it was pointed out that the small vector and scalar potentials in the QMC model are due to the assumption that the bag constant does not change in the nuclear environment [8,9]. By introducing a density-dependent bag constant it was demonstrated that large scalar and vector potentials can be produced. A necessary condition is that the value of the bag constant in the nuclear environment significantly drop below its free-space value. As a consequence relativistic nuclear phenomenology can be recovered from a modified quark-meson coupling (MQMC) model [8].

The central issue of the MQMC model is the density dependence of the bag constant. This density dependence is not known *a priori* and the idea of the MQMC model is to parametrize the bag constant and to determine the parameters by calibrating to observed nuclear properties. Two different model types have been proposed [8,9]: a direct coupling

model in which the bag constant is a function of the scalar field and a scaling model in which the bag constant is related to the effective nucleon mass. The density dependence is then generated self-consistently in terms of these in-medium quantities. By using more general parametrizations for the bag constant we refined these models in Ref. [10] and demonstrated that the MQMC model can be accurately calibrated to produce the empirical saturation properties of nuclear matter. Most importantly, the model leads to small values for the effective mass around $M^*/M \sim 0.6$ which is tightly constrained by nuclear observables [20,21].

Our purpose here is to examine if the MQMC model is consistent with established results of nuclear phenomenology. This is important because the model was proposed to describe ''new'' physics beyond the standard hadronic picture in nuclear matter and finite nuclei. Based on our previous study of nuclear matter [10] the present work is mainly concerned with the description of finite nuclei. To make contact with the hadronic framework we analyze the connection between the MQMC and QHD models. By performing a redefinition of the scalar field the MQMC model can be cast in a form equivalent to a QHD-type model with a nonlinear scalar potential and a nonlinear coupling to the gradients of the scalar field. It is well known that nonlinear scalar self-interactions must be included in relativistic mean-field models to achieve a realistic description of nuclear phenomena [22–28]. In principle, if the density dependence of the bag constant was known, the connection between the MQMC and QHD models could be used to predict the form of the nonlinear self-interactions. Furthermore, it implies that a calibration on the hadronic level, i.e., determining the nonlinear parameters, is equivalent to the calibration of the density dependence of the bag constant [10].

Although the model loses some of its predictive power, the concept of a density-dependent bag constant is useful. The original idea of the QMC model was to calibrate the model in free space such that the nucleon mass is reproduced and then to extrapolate to many-nucleon systems. Moreover, attempts have been made to describe all the relevant degrees of freedom, i.e., nucleons and mesons, within the underlying bag model [14,16]. The idea is appealing; however, it is not possible to account for all the necessary degrees of freedom. Most importantly, the scalar field which describes the midrange part of the nucleon-nucleon interaction cannot be described in the framework of the simple bag model, but it must be included. This gives rise to new parameters which cannot be determined on a fundamental level [14]. On the other hand, in the MQMC model these new parameters arise naturally from the density dependence of the bag constant.

To study properties of finite nuclei we adopt model $\mathrm{MQMC_A}$ from Ref. [10], in which the bag constant is a function of the scalar field only. For comparison we employ a QHD model that includes quartic and cubic scalar self-interactions. Relativistic mean-field models of this type reproduce the observed properties of nuclear matter and give a realistic description of the bulk properties of nuclei throughout the Periodic Table [22–28]. We calibrate the model parameters so that the MQMC and QHD models lead to the same nuclear matter properties at equilibrium.

The main difference between the MQMC and QHD models arises from the nonlinear coupling to the gradient of the scalar field which is generated by the field redefinition. This term does not contribute in nuclear matter and it mainly effects the nuclear shape leading to a more diffuse surface in the MQMC model. We compensate for this effect by adjusting the scalar mass to reproduce the experimental value of the charge radius in ^{40}Ca. After the adjustment the MQMC and QHD models are in very close agreement. The analysis of the bulk properties of closed-shell nuclei demonstrates that the MQMC model gives a realistic description of binding energies and radii. Compared to calculations based on the original QMC model [11–14] we find significant improvement, in particular for the binding energies of the light nuclei. The poor reproduction of single-particle spectra and spin-orbit splittings is the main shortcoming of the original QMC model and the study of these quantities is crucial for the present analysis. We find that the MQMC model systematically corrects these shortcomings and leads to a realistic description of the single-particle levels and spin-orbit splittings. The key observations in this success is that the MQMC model can be accurately calibrated to reproduce small values for the effective mass, which is strongly correlated with the spin-orbit force in relativistic mean-field models.

The discussion of the bulk and single-particle properties of finite nuclei demonstrates that the MQMC model provides a simple framework for describing nuclear phenomena, which incorporates quark degrees of freedom and reproduces established results. This success provides a solid foundation for the investigation of the internal nucleon structure and changes caused by the nuclear environment. An important quantity here is the nucleon size. There are several indications in nuclear phenomenology that nucleons ''swell'' in the nuclear environment. For example, the EMC effect can be explained by assuming an increased confinement size in the nuclear medium [29,30]. We analyze the average bag radius for different nuclei, which can be used to estimate the average confinement size [31]. Depending on the mass number of the nucleus the average bag radius increases substantially, up to 40% of its free space value.

The outline of this paper is as follows: In Sec. II, we present the formalism for finite nuclei. Section III contains a short summary of the QMC model and the relations which determine the properties of the nucleon. We also briefly discuss the calibration procedure. In Sec. IV, we apply our model to finite nuclei. We compare our results with QHD and with the original version of the QMC model. Section V contains a short summary.

II. DESCRIPTION OF FINITE NUCLEI

To study the properties of finite nuclei we use a relativistic mean-field model containing nucleons, neutral scalar (ϕ) and vector fields (V_μ), the isovector ρ meson field ($\mathbf{b}_\mu$), and the electromagnetic field (A_μ). We assume the nucleons obey the Dirac equation

$$\left(i\partial\!\!\!/ - \mathcal{V}\!\!\!/ - \frac{1}{2}\boldsymbol{\tau}\cdot\mathcal{B}\!\!\!/ - \frac{1}{2}(1+\tau_3)\mathcal{A}\!\!\!/ - M^* \right)\psi_N(x) = 0. \quad (1)$$

The potentials ($\mathcal{V}^\nu, \boldsymbol{\mathcal{B}}^\nu, \mathcal{A}^\nu$) and the effective mass M^* are functionals of the meson mean fields; their form depends on the underlying quark model.

In the QMC model the quarks are described by the Dirac equation

$$\left(i\partial\!\!\!/ - g_{\mathrm{v}}^{q} \mathcal{V}\!\!\!/ - \frac{1}{2} g_{\rho}^{q} \boldsymbol{\tau} \cdot \mathcal{B}\!\!\!/ - (1+3\tau_3)\frac{e}{6} \mathcal{A}\!\!\!/ - [m_q - g_{\mathrm{s}}^{q}\phi] \right) \psi_q(x) = 0, \tag{2}$$

where m_q is the current quark mass. The quark wave function is subject to the bag model boundary conditions at the surface of the bag. Because quarks and nucleons interact with the meson mean fields, Eqs. (1) and (2) define a self-consistent scheme for the description of the nuclear system. In practice, however, this entails a complicated task. The main difficulty arises from the variation of the meson mean fields over the bag volume. In consequence, the quark wave function and the ground state of a bound nucleon are no longer spherically symmetric [13]. To make a numerical solution feasible it is necessary to calculate the quark properties by using some suitable averaged form for the meson mean fields. Here we adopt the prescription of [11,12,14] and replace the meson mean fields on the quark level by their value at the center of the nucleon bag; i.e., we neglect the spatial variation of the mean fields over the bag volume. In this local density approximation the potentials in Eq. (1) are simply obtained by the corresponding nuclear matter relations, which are given by [12]

$$\mathcal{V}^{\nu} = 3 g_{\mathrm{v}}^{q} V^{\nu} \equiv g_{\mathrm{v}} V^{\nu}, \tag{3}$$

$$\boldsymbol{\mathcal{B}}^{\nu} = g_{\rho}^{q} \mathbf{b}^{\nu} \equiv g_{\rho} \mathbf{b}^{\nu}, \tag{4}$$

$$\mathcal{A}^{\nu} = e A^{\nu}. \tag{5}$$

The effective mass is an ordinary function of the scalar field, i.e.,

$$M^{*} = M^{*}(\phi). \tag{6}$$

As shown in Ref. [13], the variation of the meson mean fields over the bag volume can be taken into account perturbatively, but the effect is small. This is supported by the observation that the bag radius is maximal in the interior region of the nucleus where the gradients of the mean fields are small.

If we restrict considerations to spherically symmetric nuclei only, the V_0 component of the neutral vector field and the neutral ρ meson field (denoted by b_0) contribute. The ground state energy of a nucleus can be written as

$$E_N = \sum_{i=\mathrm{occ}} E_i + \frac{1}{2}\int dV \big([(\nabla\phi)^2 + m_{\mathrm{s}}^2\phi^2] - [(\nabla V_0)^2 + m_{\mathrm{v}}^2 V_0^2] - [(\nabla b_0)^2 + m_{\rho}^2 b_0^2] - (\nabla A_0)^2 \big), \tag{7}$$

where E_i are the eigenvalues of the Dirac equation (1). The actual mean-field configuration is obtained by extremization of the energy. This leads to the set of self-consistency equations

$$(\Delta - m_{\mathrm{s}}^2)\phi = \frac{\partial}{\partial\phi} M^{*}(\phi)\rho_{\mathrm{s}}, \tag{8}$$

$$(\Delta - m_{\mathrm{v}}^2) V_0 = -g_{\mathrm{v}}\rho, \tag{9}$$

$$(\Delta - m_{\rho}^2) b_0 = -g_{\rho}\frac{1}{2}\rho_3, \tag{10}$$

$$\Delta A_0 = -e\rho_p. \tag{11}$$

The densities on the right-hand side are the nuclear densities calculated with the wave functions in Eq. (1):

$$\rho_{\mathrm{s}} = \sum_{i=\mathrm{occ}} \overline{\psi}_N^i \psi_N^i, \tag{12}$$

$$\rho = \sum_{i=\mathrm{occ}} \overline{\psi}_N^i \gamma^0 \psi_N^i, \tag{13}$$

$$\rho_3 = \sum_{i=\mathrm{occ}} \overline{\psi}_N^i \tau_3 \gamma^0 \psi_N^i, \tag{14}$$

$$\rho_p = \frac{1}{2}\sum_{i=\mathrm{occ}} \overline{\psi}_N^i (1+\tau_3)\gamma^0 \psi_N^i. \tag{15}$$

The details of the underlying quark substructure are entirely contained in the expression for the effective mass $M^{*}(\phi)$. In the next section we will discuss the functional form of the effective mass in the framework of the QMC model.

III. QUARK-MESON COUPLING MODEL

In this section, we briefly summarize the relations which determine the nucleon properties in the quark-meson coupling model. For further details we refer the reader to Refs. [6,8,9]. According to the local density approximation, assuming constant meson mean fields in the bag volume, the energy of a bag consisting of three quarks in the ground state can be expressed as

$$E_{\mathrm{bag}} = 3\frac{\Omega_q}{R} - \frac{Z}{R} + \frac{4}{3}\pi R^3 B, \tag{16}$$

where the parameter Z accounts for the zero-point motion and B is the bag constant. The coupling of the quarks to the scalar field is inherent in the quantities Ω_q and x which are given by

$$\Omega_q = \sqrt{x^2 + (R m_q^{*})^2}, \tag{17}$$

$$j_0(x) = \left(\frac{\Omega_q - R m_q^{*}}{\Omega_q + R m_q^{*}} \right)^{1/2} j_1(x),$$

and where $m_q^{*} = m_q - g_{\mathrm{s}}^{q}\phi$ denotes the effective quark mass. For simplicity we work in the chiral limit, i.e., $m_q = 0$.

To remove the spurious center-of-mass motion in the bag we follow Ref. [5] and subtract the average value of the square momenta of the three quarks in the bag. The effective nucleon mass is then given by

$$M^{*} = \sqrt{E_{\mathrm{bag}}^2 - 3x^2/R^2}. \tag{18}$$

Alternatively, a phenomenological c.m. correction incorporated by adjusting the parameter Z can be used. In the origi-

TABLE I. Equilibrium properties of nuclear matter.

$(k_F)^0$	ρ^0	M_0^*/M	e_0	K_0	a_4
1.3 fm^{-1}	0.1484 fm^{-3}	0.63	−15.75 MeV	224.2 MeV	35 MeV

nal version of the QMC model this prescription leads to slightly bigger scalar and vector potentials [11]. However, as discussed in Ref. [10], the two different prescriptions are essentially equivalent in our generalized version of the model.

For a fixed meson mean-field configuration the bag radius R is determined by the equilibrium condition for the nucleon bag in the medium:

$$\frac{\partial M^*}{\partial R}=0. \tag{19}$$

In free space M can be fixed at its experimental value 939 MeV and the condition (19) to determine the parameters $B=B_0$ and $Z=Z_0$. For our choice, $R_0=0.6$ fm, the results for $B_0^{1/4}$ and Z_0 are 188.1 MeV and 2.03, respectively.

In the original version of the QMC model [4–6] the bag parameters B and Z were held fixed at their free-space values $B=B_0$, $Z=Z_0$. Formally, the bag constant B is associated with the QCD trace anomaly. In the nuclear environment it is expected to decrease with increasing density as argued in Ref. [32].

To account for this physics in the QMC approach Jin and Jennings [8,9] proposed two models for the medium modification of the bag constant: a direct coupling model in which the bag constant is a function of the scalar field and a scaling model which relates the bag constant directly to the effective nucleon mass. The density dependence is then generated self-consistently in terms of these in-medium quantities. In a previous work [10] we generalized this approach and demonstrated that the resulting improved MQMC model can be accurately calibrated to predict the empirical properties of nuclear matter.

For our purpose here we adopt the model MQMC$_A$ of Ref. [10] in which the bag constant depends on the scalar field only:

$$\frac{B}{B_0}=\left(1-g_B\frac{\phi}{M}F(\phi)\right)^{\kappa} \quad \text{with} \quad F(0)=1. \tag{20}$$

We model the functional form of F by using a simple polynomial parametrization

$$F(\phi)=1+\alpha\phi+\beta\phi^2. \tag{21}$$

Because the parameters B_0 and Z are fixed to reproduce the nucleon mass in the vacuum, the model contains eight free parameters. The parametrization of the bag constant contains the parameter κ and the three couplings (g_B,α,β); in addition values for the couplings g_s^q, g_v, g_ρ and for the mass of the scalar meson m_s are needed. The masses of the remaining mesons are fixed at their experimental values $m_v=783$ MeV and $m_\rho=770$ MeV.

To determine the parameters we proceed as follows [10]. For given values of κ, g_s^q, and m_s we determine the couplings $(g_B,\alpha,\beta,g_v,g_\rho)$ to reproduce the equilibrium properties of nuclear matter, which are taken to be the equilibrium density and binding energy $(\rho^0,-e_0)$, the nucleon effective mass at equilibrium (M_0^*), the compression modulus (K_0), and the symmetry energy (a_4). The equilibrium properties used here are listed in Table I. For more details concerning the calibration procedure we refer the reader to Ref. [10].

The set of equations, Eq. (1) and Eqs. (8)–(11), in combination with the expression for the effective mass in Eq. (18) may be solved by a standard iteration procedure [33,34]. In this paper the numerical calculation was carried out by using a modified version of the program TIMORA described in [34].

IV. PROPERTIES OF FINITE NUCLEI

As discussed in Ref. [10] for the case of nuclear matter, there is a direct relation between the MQMC model and QHD-type mean-field models. Here we will briefly review the analysis and discuss the consequences for finite systems.

The main difference between the MQMC and QHD models is the functional form of the effective mass. In the MQMC model it is a complicated function of the scalar field,

$$M^*_{\mathrm{MQMC}}=M^*_{\mathrm{MQMC}}(\phi), \tag{22}$$

whereas in QHD it is linearly related to the scalar field,

$$M^*_{\mathrm{QHD}}=M-g_0\Phi. \tag{23}$$

This suggests a redefinition of the scalar field in MQMC:

$$g_0\Phi(\phi)\equiv M-M^*_{\mathrm{MQMC}}(\phi)=M-\sqrt{E^2_{\mathrm{bag}}-3x^2/R^2}. \tag{24}$$

The coupling g_0 is chosen to normalize the new field according to

$$\Phi(\phi)\underset{\phi\to 0}{=}\phi+O(\phi^2),$$

and is given by

$$g_0=-\left.\frac{\partial M^*(\phi)}{\partial\phi}\right|_{\phi=0}. \tag{25}$$

The contribution of the scalar field to the energy in Eq. (7) can now be expressed in terms of the new field

$$E_s=\frac{1}{2}\int dV[(\nabla\phi)^2+m_s^2\phi^2] \tag{26}$$

$$=\int dV\left[\frac{1}{2}(\nabla\Phi)^2h(\Phi)^2+U_s(\Phi)\right],$$

with a nonlinear scalar potential

$$U_s(\phi) \equiv \frac{1}{2} m_s^2 \phi^2(\Phi) \tag{27}$$

and with

$$h(\Phi) = \frac{\partial \phi}{\partial \Phi} = -\frac{g_0}{\partial M^*/\partial \phi}. \tag{28}$$

The self-consistency equation for the scalar field, Eq. (8), is replaced by

$$h^2 \Delta \Phi + h \frac{\partial h}{\partial \Phi} (\nabla \Phi)^2 - \frac{1}{2} \frac{\partial U_s}{\partial \Phi} = -g_0 \rho_s. \tag{29}$$

Formulated in terms of the new field Φ the MQMC model is of the same form as a QHD model with a nonlinear scalar potential $U_s(\Phi)$ and with a coupling $h(\Phi)$ to the gradients of the scalar field.

The standard form of the nonlinear scalar potential is [22]

$$U_s(\Phi) = \frac{1}{2} m_s^2 \Phi^2 + \frac{\kappa}{6} \Phi^3 + \frac{\lambda}{24} \Phi^4. \tag{30}$$

The coupling $h(\Phi)$ has no effect in nuclear matter calculations and is not included in conventional QHD models. From a modern point of view, our model contains a subset of possible nonlinear meson-meson couplings. In more sophisticated versions of QHD [21,35], inspired by concepts and methods of effective field theory, these terms and many others are considered. However, rather than attempting to compete with these models, it is our goal to analyze if an approach which is based on a simple quark model can reproduce well-established results of nuclear phenomenology. For comparison we employ a conventional version of QHD which contains the standard form of the nonlinear potential given by Eq. (30) and which does not include the coupling $h(\Phi)$. It is well established that relativistic mean-field models of this type provide a realistic description of the bulk properties of finite nuclei and nuclear matter [19,22–28]. For the parameters we chose the set NLC of Ref. [24]. It was obtained by fitting to empirical saturation properties of nuclear matter and to bulk properties of finite nuclei. In nuclear matter this parameter set leads to the equilibrium properties listed in Table I. The value of the scalar mass which was determined to reproduce the charge radius of ^{40}Ca is $m_s = 500.8$ MeV. As discussed in the last section we calibrate the MQMC model to produce exactly the same nuclear matter properties.

The main difference between the two models arises from the coupling $h(\Phi)$ which is indicated in Fig. 1 for $\kappa = 4$ and for various values of g_s^q. The coupling becomes more important for increasing values of g_s^q. Relevant for applications to finite nuclei is the region below $g_0\Phi = 350$ MeV which corresponds roughly to the saturation point of nuclear matter. In that region the shape of the function $h(\Phi)$ depends only weakly on the model parameters. This changes drastically at higher values of the scalar field which corresponds to high densities. The predicted nonlinear scalar potential, Eq. (27), is indicated in Fig. 2. We also show the corresponding QHD potential. Below $g_0\Phi = 500$ MeV the different curves are almost indistinguishable [10]. Similar as we observed in the previous figure, the curves deviate at large values of the scalar field.

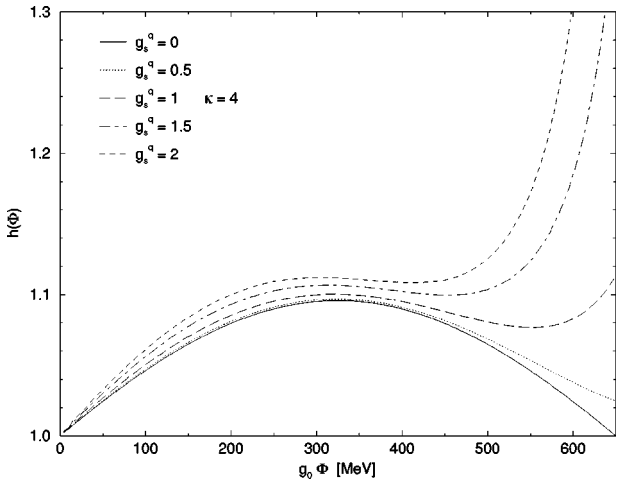

FIG. 1. Gradient coupling $h(\Phi)$ as a function of the transformed scalar field $g_0\Phi = M - M^*$ calculated with $\kappa = 4$ and for various values of g_s^q.

The most prominent effect of the coupling $h(\Phi)$ is changes of the nuclear surface. This can be studied in Fig. 3 which indicates the baryon density for ^{208}Pb. We compare the MQMC results for two different scalar masses with QHD. As indicated by the dotted line, the density in the interior region is smaller and the surface more diffuse if the same scalar mass is used as in QHD. To compensate this effect we adjusted the scalar mass such that our model reproduces the charge radius of ^{40}Ca. For the parametrization in Fig. 3 this leads to a value of $m_s = 546.5$ MeV. The corresponding density is indicated by the dashed line.

Charge densities and charge radii are calculated by convoluting the point proton density, Eq. (15), with an empirical proton charge form factor [33]. As an alternative we determine the charge density by using the prediction of the MQMC model for the charge distribution of the proton $\rho_c^{\rm bag}$:

$$\rho_c(\mathbf{x}) = \int d^3y \rho_c^{\rm bag}[\mathbf{x} - \mathbf{y}, R(\mathbf{y})] \rho_p(\mathbf{y}), \tag{31}$$

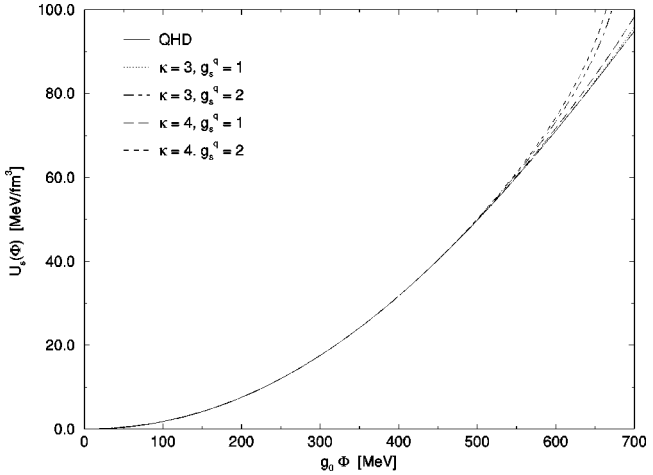

FIG. 2. Predicted nonlinear scalar potential as a function of the transformed scalar field $g_0\Phi = M - M^*$ for different parameters κ and g_s^q. In addition the QHD potential is also indicated.

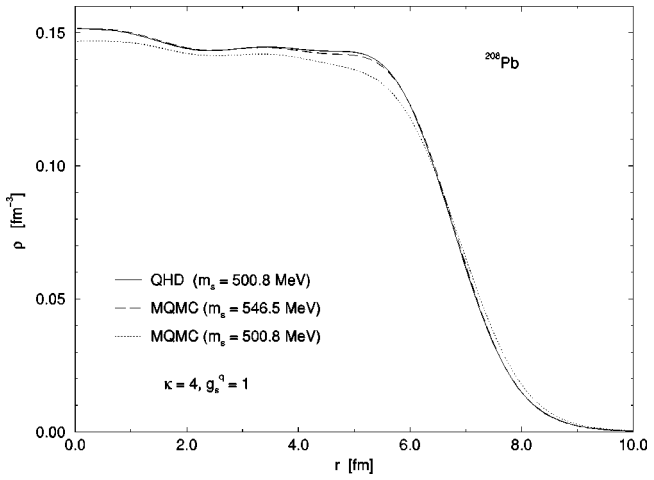

FIG. 3. Baryon density for ^{208}Pb calculated with two different values of the scalar mass m_s. The QHD result is also indicated.

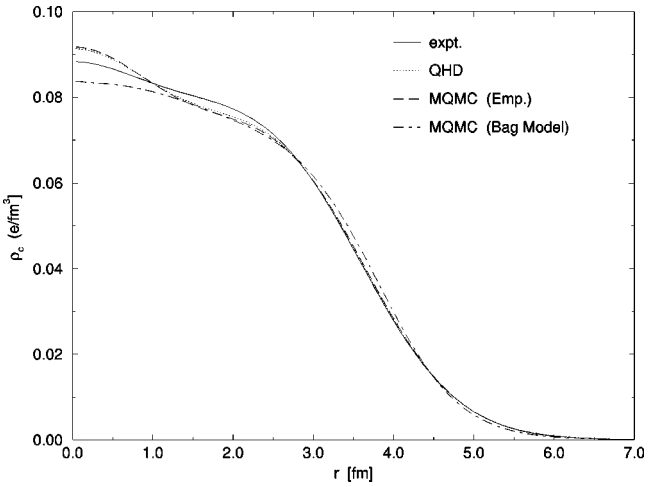

FIG. 4. Charge density for ^{40}Ca. The curves for the MQMC model are calculated using an empirical proton charge form factor (dashed curve) and the proton charge distribution predicted by the bag model (dash-dotted curve). We also show the QHD result and the experimental charge density. The MQMC parameters are $\kappa = 4$ and $g_s^q = 0$.

with

$$\rho_c^{\rm bag}[\mathbf{x},R] = \psi_q^{R\dagger}(\mathbf{x})\psi_q^R(\mathbf{x})\Theta(R-|\mathbf{x}|). \tag{32}$$

The subscript R indicates that the quark wave functions in Eq. (2) depend explicitly on the bag radius. Note that the bag radius is a function of the density, which has to be taken into account when performing the integral in Eq. (31). The results are indicated in Fig. 4. For the empirical form factor the MQMC prediction is very close to the QHD result. Typically the curves slightly overestimate the experimental charge density [36] in the interior region. The bag-model form factor leads to a density which is too small in the interior region and too high at the surface of the nucleus. This is because the bag radius is maximal in the center of the nucleus and decreases with decreasing density [8–10]. The calculated rms charge radius for this case is $r_c = 3.44$ fm, thus only slightly smaller than for the other curves ($r_c = 3.48$ fm). Although our simple version of the bag model is too crude to give a realistic description of electromagnetic form factors, it is interesting to observe the consequences of the increased nucleon size for the bulk properties of finite nuclei.

Binding energies and rms charge radii for ^{16}O, ^{40}Ca, ^{90}Zr, and ^{208}Pb are shown in Table II for various values of κ and g_s^q. Also included are the QHD results, the experimental values and results based on the original QMC model taken from Refs. [12,14] and [13]. Overall the MQMC model gives a realistic description of the binding energies and radii. We observe a small model dependence. Because of changes in the surface systematic, the binding energies increase with κ and g_s^q. Small values of the parameters lead to a steeper surface region. Correspondingly, the gradient contributions of the mean fields to the energy in Eq. (7) increase whereas the energy levels of the nucleons change only marginally. Generally, the QHD and MQMC models lead to similar predictions. We find the largest deviation of roughly 8% for the binding energies of the lightest nuclei. The parameter set with $\kappa = 4$ and $g_s^q = 2$ gives the best agreement with the experimental numbers.

Among the different models used in Refs. [12,14] and [13] we have chosen the ones which yield the best reproduction of the experimental data. Model A1 from [13] includes a perturbative correction which accounts for the variation of the meson mean fields inside the nucleon bag. The results for model A1 from [13] as well as the results from Refs. [12,14]

TABLE II. Binding energy per nucleon e_N (in MeV) and rms charge radius r_c in (fm) for several closed shell nuclei. The results for models A1 and QMC are taken from Ref. [13] and Refs. [12,14], respectively.

Model		m_s	^{16}O		^{40}Ca		^{90}Zr		^{208}Pb	
κ	g_s^q	(MeV)	e_N	r_c	e_N	r_c	e_N	r_c	e_N	r_c
3	0	540.5	-7.12	2.75	-8.10	3.48	-8.29	4.29	-7.53	5.56
3	1	542.5	-7.20	2.74	-8.13	3.48	-8.32	4.29	-7.55	5.56
3	2	549.5	-7.51	2.74	-8.37	3.48	-8.50	4.29	-7.70	5.57
4	0	545	-7.32	2.74	-8.23	3.48	-8.40	4.29	-7.62	5.56
4	1	546.5	-7.39	2.74	-8.28	3.48	-8.43	4.29	-7.64	5.56
4	2	555.5	-7.79	2.73	-8.57	3.48	-8.66	4.29	-7.81	5.57
Model A1 [13]		450	-6.22	2.75	-7.46	3.48	-7.84	4.32	-7.59	5.59
QMC [12,14]		418	-5.84	2.79	-7.36	3.48	-7.79	4.27	-7.25	5.49
QHD		500.8	-7.18	2.74	-8.14	3.48	-8.33	4.29	-7.57	5.56
Expt.			-7.98	2.73	-8.45	3.48	-8.66	4.27	-7.86	5.50

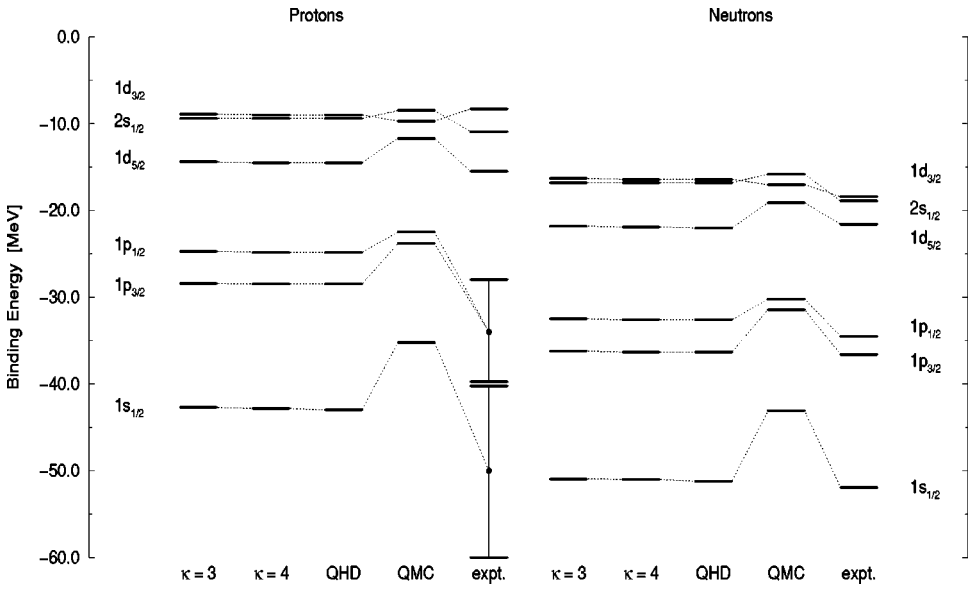

FIG. 5. Single-particle spectrum of ^{40}Ca for $\kappa=3,4$ and $g_s^q=1$. The results for the original QMC model are taken from [12,14]. We also show the QHD result and the experimental spectrum [37].

are based on the original QMC model with the bag constant held fixed in the medium. Generally these models underestimate the binding energies, most drastically for the light nuclei.

As stated in Ref. [13] the original QMC model leads to a fair description of charge radii and binding energies but gives only a poor reproduction of single-particle spectra and spin-orbit splittings. Spin-orbit splittings are highly correlated to the effective nucleon mass which is too high in the original QMC model. In view of these shortcomings the analysis of single-particle spectra and spin-orbit splittings in the MQMC model is very important. The single-particle levels for ^{40}Ca are shown in Fig. 5. The MQMC model clearly gives a more realistic description of the energy levels than the original QMC model. In particular the energies of the deeply bound states are better reproduced. Note the incorrect level ordering of the $2s_{1/2}$ and $1d_{3/2}$ sates in the QMC model [12,14]. We observe only a weak model dependence and a very good agreement between QHD and MQMC. This is in accordance with the observation that the gradient coupling $h(\Phi)$, which is not included in the present version of QHD, has only a small effect on the single-particle energies. Results for other nuclei are similar. Spin-orbit splittings for the highest occupied proton and neutron sates in ^{208}Pb are shown in Table III. The results demonstrate directly the effect of the density-dependent bag constant. The QMC model systematically underpredicts the splittings [12]. The small value of the effective mass in the MQMC model significantly corrects this shortcoming.

Up to this point our analysis was mainly concerned with bulk and single-particle properties of nuclei. We have established that the MQMC model provides a realistic description of these quantities and we now turn to the internal nucleon structure. One of the main features of the MQMC model is the density-dependent bag constant. Decreasing the bag constant below its free-space value leads to an increase of the bag radius in the nuclear environment. To achieve nuclear saturation for values of the effective mass in the range $0.6 \lesssim M^*/M \lesssim 0.7$ requires the bag constant to drop substantially, leading to sizable changes in the bag radius [8–10].

The nucleon size is an important phenomenological quantity in many nuclear physics issues. Evidence that the nucleon size changes in the nuclear medium comes mainly from quasielastic electron-nucleus scattering. For example, the depletion of the nucleons structure function in the medium Bjorken x region, i.e., the EMC effect, can be explained by assuming an increased confinement size of quarks and gluons in a nucleus.

In the so-called dynamical rescaling analysis of the EMC effect one assumes that the structure function of a nucleon in the nuclear environment is related to that of a free nucleon by rescaling the momentum dependence [29,30]. The rescaling parameter is determined by the extent to which the confinement size for a nucleon in the nuclear medium changes. Based on the dynamical rescaling assumption, the EMC effect was studied in the framework of the MQMC model [31]. For a nucleus the change of the confinement size can be estimated in terms of the ratio $\overline{R_A}/R_0$ where R_0 is the bag

TABLE III. Spin-orbit splittings of the highest occupied proton and neutron levels in ^{208}Pb. For the MQMC model the scalar coupling to the quarks is $g_s^q=1$.

Protons		$\kappa=3$	$\kappa=4$	QHD	QMC [12]	Expt. [37]
$\Delta E(2d_{5/2}-2d_{3/2})$	(MeV)	-1.42	-1.41	-1.39	-0.6	-1.3
$\Delta E(1g_{9/2}-1g_{7/2})$	(MeV)	-3.40	-3.40	-3.43	-1.3	-4.0
Neutrons		$\kappa=3$	$\kappa=4$	QHD	QMC [12]	Expt. [37]
$\Delta E(3p_{3/2}-3p_{1/2})$	(MeV)	-0.68	-0.68	-0.66	-0.3	-0.9
$\Delta E(2f_{7/2}-2f_{5/2})$	(MeV)	-1.80	-1.78	-1.74	-0.8	-1.8

TABLE IV. Average bag radius $\overline{R_A}/R_0$.

Model		^{16}O	^{40}Ca	^{90}Zr	^{208}Pb	Nuclear matter
κ	g_s^q	$\overline{R_A}/R_0$	$\overline{R_A}/R_0$	$\overline{R_A}/R_0$	$\overline{R_A}/R_0$	$\overline{R_A}/R_0$
3	0	1.33	1.38	1.42	1.42	1.59
3	1	1.27	1.31	1.34	1.34	1.47
3	2	1.22	1.26	1.28	1.28	1.39
4	0	1.33	1.38	1.42	1.42	1.59
4	1	1.27	1.31	1.34	1.34	1.47
4	2	1.23	1.26	1.28	1.28	1.39

radius in the vacuum and $\overline{R_A}$ is the average bag radius in the nucleus given by

$$\overline{R_A}=\frac{\int d^3r R[\rho(r)]\rho(r)}{\int d^3r \rho(r)}. \tag{33}$$

The analysis of the ratio $\overline{R_A}/R_0$ in Ref. [31] was based on using phenomenological fits for the nuclear density distributions. Here we will present a consistent calculation of Eq. (33) with nuclear densities generated within the MQMC model. The predictions for $\overline{R_A}/R_0$ are listed in Table IV. As expected the average bag radius increases with the number of nucleons. For comparison the corresponding ratios for infinite nuclear matter at the saturation point are also included in the last row of Table IV. The effect of the increased nucleon size is more pronounced for zero and small values of the scalar-quark coupling in agreement with our findings for nuclear matter [10]. The predictions for the radii are roughly 10–20 % bigger than the results of Ref. [31]. This is mainly because the value of the effective mass is higher in their version of the model ($M^*/M\sim 0.72$). Generally, our ratios are higher than the numbers quoted in the literature to explain the EMC effect [30]. Recently, the medium dependence of the nucleon size was examined in a sightly different context [38]. Based on the original version of the MQMC model [8,9] a limit for the reduction of the bag constant was obtained by using constraints from quasielastic electron-nucleus scattering data. The reduction of the bag constant was estimated to be roughly 10–15 % which implies values for the effective nucleon mass around $M^*/M\sim 0.75$ and an increase of the bag radius smaller than 5%.

Although our predictions for the nucleon size seem to be too large, one has to be careful in drawing conclusions. In the context of electron-nucleus scattering it is well known that different theoretical descriptions often lead to quite different interpretations. For example, the y-scaling analysis [39] reproduces many features of the existing data assuming a fixed nucleon size. In our work we have demonstrated that the MQMC model provides a simple framework for describing nuclear phenomena, which incorporates quark degrees of freedom and reproduces established results. In principle, we could decrease the ratios $\overline{R_A}/R_0$ even further by using larger values for g_s^q at the expense of too large binding energies and radii. The problem rests on the correlation between the effective mass and the value of the bag constant. To achieve a realistic description of nuclear matter and finite nuclei the bag constant in the medium has to be significantly lower than in free space. Thus, in the framework of the MQMC model successful nuclear phenomenology leads to large nucleon radii.

To resolve the discrepancy between our predictions for the nucleon size and the results constrained by quasielastic electron-nucleus scattering further studies are necessary. For example, the uncertainties of the dynamical rescaling approach are difficult to estimate. Instead of combining the predictions for the changes of the internal quark structure with other models it is more consistent to investigate the medium modifications of the nucleon structure function directly. On basis of the QMC model such studies were reported in Refs. [40–42]. In these works the resolution scale has been fixed at its value for free nucleons because the bag radius in the original QMC changes only marginally in nuclear matter. The medium modification of the structure function arises mainly from kinematic effects due to the scalar and vector mean fields. Further studies are needed which take into account the effect of the decreasing bag radius. This will provide a more consistent test of the predictive power of the MQMC model and is an important topic for future investigations.

V. SUMMARY

In this paper we study properties of finite nuclei based on the modified quark-meson coupling model. This model describes nucleons as nonoverlapping MIT bags interacting through scalar and vector mean fields. Of central importance is the bag constant which we assume to depend on the density of the nuclear environment. We employ a model for the bag constant in which the density dependence is parametrized in terms of the scalar mean field. The unknown model parameters can be fit to properties of nuclear matter near equilibrium that are known to be characteristic of the observed bulk and single-particle properties of nuclei.

By performing a redefinition of the scalar field we demonstrate that the resulting energy functional corresponds to a QHD-type, hadronic mean-field model with nonlinear scalar self-interactions.

Our basic goal is to study properties of finite nuclei. We investigate whether the MQMC model leads to results which are consistent with established hadronic models. This is relevant in view of the hope of applying quark models to describe ''new'' physics which goes beyond the hadronic picture.

In general, we find that the MQMC model provides a realistic description of the bulk properties and single-particle spectra of closed-shell nuclei and is a significant improvement over the original QMC model. The predictions for single-particle spectra are more realistic and the binding energies of the light nuclei are better reproduced. This is the direct result of the MQMC model accurately reproducing the effective nucleon mass which is strongly correlated to the spin-orbit force in finite nuclei. In contrast, the quantity predicted by the original QMC model is too high.

To make contact with the established hadronic framework we compare our results with a QHD model including quartic

and cubic scalar self-interactions. The MQMC and QHD models are calibrated to produce the same equilibrium properties of nuclear matter. Generally, the predictions of the two models are very similar. Differences arise mainly from a nonlinear coupling to the gradients of the scalar field which is not included in the employed version of QHD. This coupling effects the shape of the nuclei, leading to a more diffuse surface in the MQMC model.

The nuclear matter studies of Ref. [10] and the present analysis of finite nuclei demonstrate that the MQMC model provides a simple framework for describing nuclear phenomena, which incorporates quark degrees of freedom and reproduces established results. Based on this success we can now start investigating changes of the internal nucleon structure in the nuclear environment. Guided by previous studies [31] we analyzed the average bag radius in different nuclei which can be used to estimate medium modifications of the nucleon confinement size. This quantity is an important input in the dynamical rescaling analysis of the EMC effect. We find average bag radii which increase up to 40% of the free-space value. These predictions are too big when compared to the numbers quoted in the literature [30,31,38]. However, our predictions are a direct consequence of successful nuclear phenomenology. Therefore we believe it is necessary to study the nucleon structure function directly on basis of the MQMC model before conclusions can be drawn.

ACKNOWLEDGMENTS

We thank B. K. Jennings and H. M. Saldaña for useful comments. This work was supported by the Natural Science and Engineering Research Council of Canada.

[1] For a review, see M. Arneodo, Phys. Rep. **240**, 301 (1994).
[2] For a recent review, see R. Alkofer, H. Reinhardt, and H. Weigel, Phys. Rep. **265**, 139 (1996).
[3] For example, see J. Achtzehnter, W. Scheid, and L. Wilets, Phys. Rev. D **32**, 2414 (1985).
[4] P. A. M. Guichon, Phys. Lett. B **200**, 235 (1988).
[5] S. Fleck, W. Bentz, K. Shimizu, and K. Yazaki, Nucl. Phys. **A510**, 731 (1990).
[6] K. Saito and A. W. Thomas, Phys. Lett. B **327**, 9 (1994).
[7] K. Saito and A. W. Thomas, Phys. Rev. C **52**, 2789 (1995).
[8] X. Jin and B. K. Jennings, Phys. Lett. B **374**, 13 (1996).
[9] X. Jin and B. K. Jennings, Phys. Rev. C **54**, 1427 (1996).
[10] H. Müller and B. K. Jennings, Nucl. Phys. **A626**, 966 (1997).
[11] P. A. M. Guichon, K. Saito, E. Rodionov, and A. W. Thomas, Nucl. Phys. **A601**, 349 (1996).
[12] K. Saito, K. Tsushima, and A. W. Thomas, Nucl. Phys. **A609**, 339 (1996).
[13] P. G. Blunden and G. A. Miller, Phys. Rev. C **54**, 359 (1996).
[14] K. Saito, K. Tsushima, and A. W. Thomas, Phys. Rev. C **55**, 2637 (1997).
[15] P. A. M. Guichon, K. Saito, and A. W. Thomas, Aust. J. Phys. **50**, 115 (1997).
[16] K. Saito and A. W. Thomas, Phys. Rev. C **51**, 2757 (1995).
[17] K. Tsushima, K. Saito, and A. W. Thomas, Phys. Lett. B **411**, 9 (1997).
[18] K. Tsushima, K. Saito, J. Haidenbauer, and A. W. Thomas, Report No. ADP-97-26-T-261, 1997.
[19] For an updated status report, see B. D. Serot and J. D. Walecka, Int. J. of Mod. Phys. E (to be published).
[20] R. J. Furnstahl, H.-B. Tang, and B. D. Serot, Phys. Rev. C **52**, 1368 (1995).
[21] R. J. Furnstahl, B. D. Serot, and H.-B. Tang, Nucl. Phys. **A598**, 539 (1996).
[22] J. Boguta and A. R. Bodmer, Nucl. Phys. **A292**, 413 (1977).
[23] P. G. Reinhard, M. Rufa, J. Maruhn, W. Greiner, and J. Friedrich, Z. Phys. A **323**, 13 (1986).
[24] R. J. Furnstahl, C. E. Price, and G. E. Walker, Phys. Rev. C **36**, 2590 (1987).
[25] R. J. Furnstahl and C. E. Price, Phys. Rev. C **40**, 1398 (1989).
[26] A. R. Bodmer and C. E. Price, Nucl. Phys. **A505**, 123 (1989).
[27] Y. K. Gambhir, P. Ring, and A. Thimet, Ann. Phys. (N.Y.) **198**, 132 (1990).
[28] R. J. Furnstahl and B. D. Serot, Phys. Rev. C **47**, 2338 (1993).
[29] F. E. Close, R. L. Jaffe, R. G Roberts, and G. G. Ross, Phys. Rev. D **31**, 1004 (1985).
[30] F. E. Close, Nucl. Phys. **A446**, 273c (1985).
[31] X. Jin and B. K. Jennings, Phys. Rev. C **55**, 1567 (1997).
[32] C. Adami and G. E. Brown, Phys. Rep. **234**, 1 (1993).
[33] C. J. Horowitz and B. D. Serot, Nucl. Phys. **A368**, 503 (1981).
[34] C. J. Horowitz, D. P. Murdoch, and B. D. Serot, in *Computational Nuclear Physics 1*, edited by K. Langanke, J. A. Maruhn, and S. E. Koonin (Springer, Berlin, 1991), p. 129.
[35] R. J. Furnstahl, B. D. Serot, and H.-B. Tang, Nucl. Phys. **A615**, 441 (1997).
[36] H. de Vries, C. W. de Jaeger, and C. de Vries, At. Data Nucl. Data Tables **36**, 495 (1987).
[37] X. Campi and D. W. Sprung, Nucl. Phys. **A194**, 401 (1972).
[38] D. H. Lu, K. Tsushima, A. W. Thomas, and A. G. Williams, Report No. ADP-97-45-T273, 1997.
[39] D. B. Day, J. S. McCarthy, T. W. Donnelly, and I. Sick, Ann. Rev. Nucl. Part. Sci. **40**, 357 (1990).
[40] A. W. Thomas, A. Michels, A. W. Schreiber, and P. A. M. Guichon, Phys. Lett. B **233**, 43 (1989).
[41] K. Saito, A. Michels, and A. W. Thomas, Phys. Rev. C **46**, R2149 (1992).
[42] K. Saito and A. W. Thomas, Nucl. Phys. **A574**, 659 (1994).